Maximilian Grösche[1]
Jan G. Korvink[2]
Kersten S. Rabe[1]
Christof M. Niemeyer[1,*]

Comparison of Storage Methods for Microfluidically Produced Water-in-Oil Droplets

Microfluidically produced water-in-oil droplets are an important platform for biochemical research. To investigate the structural integrity of droplets during transfer and storage processes, different methods were compared. Storage as isolated droplets inside plastic tubing or a designed microfluidic chamber led to moderate decreases in droplet volume but only slight changes in monodispersity, whereas bulk storage in an Eppendorf cup led to the complete loss of monodispersity. It is further demonstrated that on-chip storage of the droplets in a fluidic microcavity array avoids coalescence and enables a reduction in volume with the concurrent increase in the concentration of entrapped proteins, which is relevant for applications in life science.

Keywords: Microfluidics, Off-chip storage, Proteins, Vertical storage chamber, Water-in-oil droplets

1 Introduction

It is undisputed that the miniaturization of semiconductor technology has led to the continuous acceleration and perfor mance improvements of electronic devices. Continuous minia turization has made microprocessors not only more powerful but also more cost effective. The technology of microfluidics strives to transfer these developments to the fields of chemistry and biomedical sciences [1 7]. The miniaturization of conven tional reaction vessels into single droplets not only enables a considerable reduction of the reactor volume, and thus of the required sample size, but also permits better control over the temperature, and the diffusion based mixing of tiny reaction volumes can often accelerate the reactions and, in some cases, even make them possible [8, 9].

Droplet microfluidics enables the handling of very small liq uid packages, which are usually produced and processed in the form of small water in oil (W/O) droplets with volumes in the picoliter to nanoliter range. Every single W/O droplet repre sents a self contained reaction vessel generated with a typical frequency of several kilohertz [10], thus enabling the rapid pro duction of hundreds of thousands of microreactors in a very short time. The development of so called "unit operations", such as droplet splitting or combining [11 13], selective injec tion of reagents [14], mixing [15], and sorting [16], has opened the microfluidic droplet technology to a wide range of applica tions in chemistry and biology. Hereby, and by the selection of suitable oil and surfactant variants [17], numerous applications can be accomplished in microfluidic droplets, such as the syn thesis of nanoparticles [18, 19], polymerase chain reactions (PCR) [20], or cell culture experiments [21, 22].

One of the most important operations for many of these applications is sample incubation and, depending on the specif ic needs, the continuous acquisition of the course of the read out signals. Depending on the application, different require ments are imposed on the length of the incubation time and the environmental conditions. To this end, the microfluidically generated droplets are usually transferred, after chip based production, into a storage vessel (e.g., an Eppendorf cup or polymer tubing), to meet the requirements of the respective incubation variant. However, most storage solutions do not allow for continuous observation of the (bio)chemical process es inside the droplets, and it is therefore necessary to return the droplets to an observation structure or to store them on chip immediately after generation. An important aspect for the suc cess of the experiment is that the droplets retain their structural integrity both during transfer and within the incubation reser voir. Decisive factors for this are the choice of the oil surfactant system and the transfer distance in between the generation and the storage structure [17]. To shed more light on these aspects, we report here on a systematic investigation of three different

[1]Maximilian Grosche, Dr. Kersten S. Rabe, Prof. Dr. Christof M. Nie meyer
christof.niemeyer@kit.edu
Karlsruhe Institute of Technology (KIT), Institute for Biological Interfaces (IBG 1), Hermann von Helmholtz Platz 1, 76344 Eggen stein Leopoldshafen, Germany.
[2]Prof. Dr. Jan G. Korvink
Karlsruhe Institute of Technology (KIT), Institute of Microstructure Technology (IMT), Hermann von Helmholtz Platz 1, 76344 Eggen stein Leopoldshafen, Germany.

storage devices with regard to their suitability for maintaining the structural integrity of the droplets during these processes (Fig. 1). In addition, we present an on chip incubation design that enables both the structural integrity of the droplets to be maintained and the droplet volume to be controlled by evapo ration.

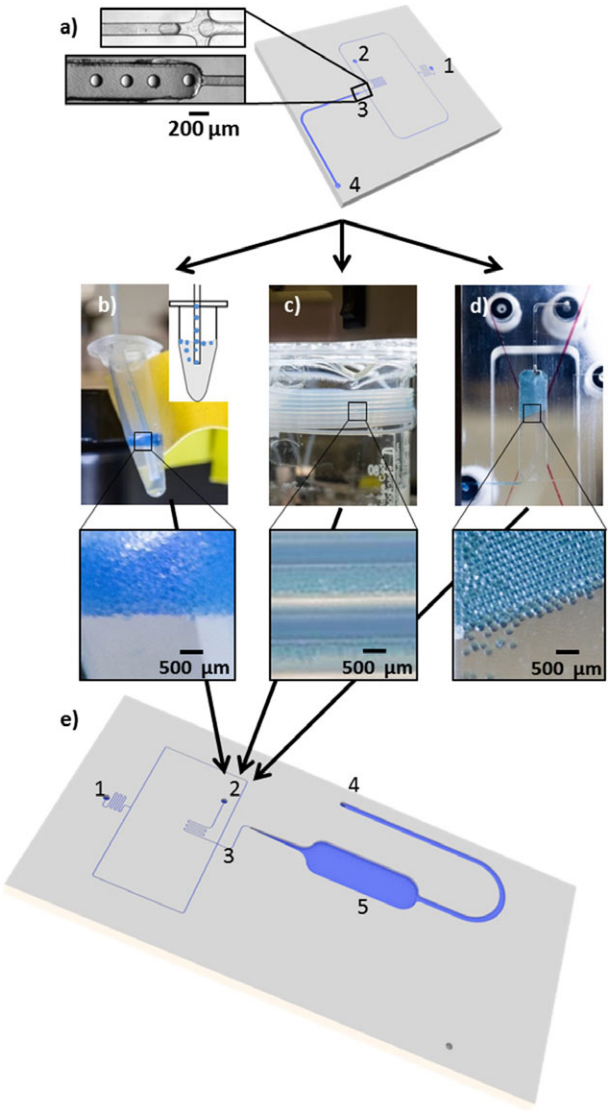

Figure 1. Schematic illustration of (a) the flow-focusing structure for W/O droplet generation containing the continuous phase inlet (1), the dispersed phase inlet (2), the droplet generation intersection (3) with a 100 µm × 100 µm cross-section (inset), and the droplet outlet (4). The outlet is designed such that the droplets can float freely in the channel (inset) to enter a storage vessel. (b d) Photographic images of the bulk storage in an Eppendorf cup (b), the PTFE tubing (di = 0.5 mm, da = 1.6 mm) for droplet storage (c), and the VDS chip made of PMMA (d). The insets show the respective storage vessels at higher magnification. (e) Schematic illustration of the OCS chamber containing a spacing phase (1), an inlet for the droplets (2), a separating intersection (3), the OCS chamber (5), and the outlet (4).

2 Experimental

The fluidic structures were designed by computer aided design (Inventor 2018, Autodesk). Casting molds were produced for all microfluidic structures using micromilling (Mini Mill GX, Minitech Machinery, USA). In a standard soft lithography step, the molds were filled with polydimethylsiloxane (PDMS). In lets and outlets were punched into the silicone with a biopsy needle. The resulting structures were bonded to PDMS patches after treatment with oxygen plasma. The microfluidic chips were connected to a syringe pump system (neMESYS, Cetoni, Germany) using polytetrafluoroethylene (PTFE) tubes.

2.1 Off-Chip Storage

The structure for the microfluidic generation of W/O drop lets is shown in Fig. 1 a. It consists of an inlet for the contin uous oil phase (1), an inlet for the dispersed aqueous phase (2), and a flow focusing intersection (3) with a cross section of 100 µm × 100 µm. The continuous phase was Novec 7500 (3M) with 2.5 % PicoSurf 1 (Dolomite Microfluidics), whereas the dispersed phase was based on deionized (DI) water sup plemented with xylenecyanol (3.4 mM) as dye for better visi bility of the aqueous phase.

The W/O droplets were generated at the intersection (Fig. 1, inset) with the flow rates Q_{cont} = 12 µL min^{-1} and Q_{disp} = 4 µL min^{-1}, and entered the respective storage struc ture via the outlet (4). The outlet had a cross section of 350 µm × 200 µm to enable measurement of the droplets with out making contact with the channel walls. The droplets were recorded by a fluorescence microscope (Zeiss Observer, Zeiss) at 1200 fps using high speed imaging (MQ003MG CM, Ximea GmbH) and their inertial volume was determined with the Fiji software [23].

The droplets were transferred via PTFE tubing into one of the three storage structures tested here (Fig. 1 b d). The first type of incubation vessels tested were 0.5 mL Eppendorf reac tion cups, in the lid of which an opening for the tubing connec tion had been drilled (Fig. 1 b). Secondly, a 100 cm long PTFE tube was used for droplet storage (Fig. 1 c). Thirdly, a designed structure made of polymethylmethacrylate (PMMA), in the fol lowing dubbed as vertical droplet storage (VDS) structure, was used for droplet storage (Figs. 1 d and 2). By employing PTFE, polypropylene (PP), and PMMA materials, which allow no or only very low gas exchange, evaporation from the tubing and off chip reservoirs should be minimal.

As shown in Fig. 2, the VDS chamber consisted of an inlet for the droplets (1), a siphon structure for excess oil (3), and an outlet (2) at the top of the chamber. Due to the higher density of the fluorocarbonated oil, the droplets rise into the chamber, preventing them from exiting the structure through the closed outlet. For droplet transfer, the oil siphon (3) was closed and an oil flow was created through the inlet. This pushed the droplets through the outlet via a PTFE tube back into the on chip storage (OCS) structure (see below). Representative images obtained during the filling process are shown in Fig. 1 d.

Subsequent to storage and analysis (described below), the droplets were transferred by reversing the flow into the OCS

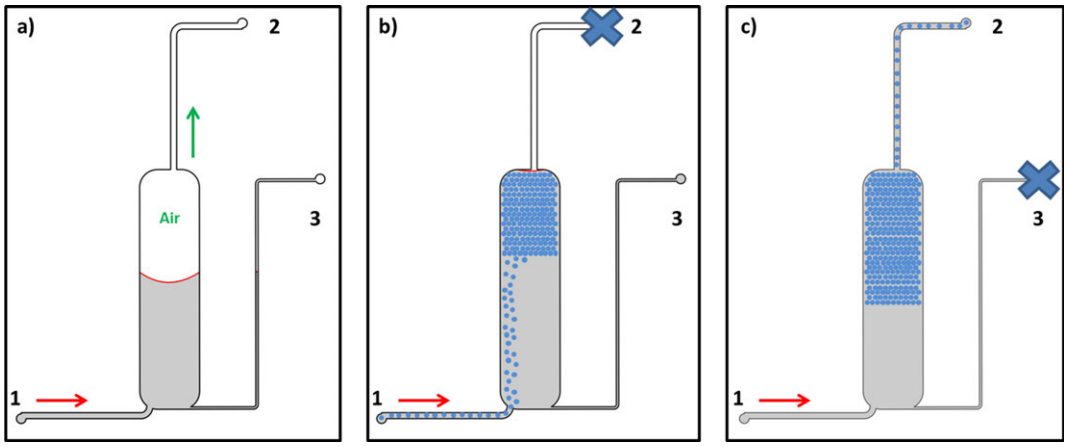

Figure 2. Operation of the VDS structure. (a) Oil is filled into the chamber from the inlet (1). Outlet (2) and siphon (3) are open. The red meniscus represents the filling level of the oil. (b) Droplet filling of the chamber: Output (2) is closed; the droplets enter the chamber through inlet (1) and ascend. Excess oil is automatically removed through the siphon (3). (c) Droplet recovery: Outlet (2) is opened and siphon (3) is closed. By introducing oil through inlet (1), the droplets are pushed out through outlet (2).

structure (Fig. 1 e). The OCS chip contained the inlet for the continuous phase (1), which was used to space the droplets at the intersection (3), whereas the dispersed phase that contained the droplets was transferred into the OCS chip via inlet (2). Therefore, the transfer of the droplets led to their packing as a monolayer in the storage chamber of the OCS structure (5), which was then subjected to microscopic analysis of the droplet volume (Zeiss Observer, Zeiss; Prime 95B camera, Photometrix, Fiji software). Although the droplets could be removed from the chamber through the outlet (4) if required, a new OCS chip was typically used for each storage experiment.

2.2 On-Chip Storage

To investigate in situ on chip storage of droplets, an OCS device (Fig. 1 e) was used that contained a structured OCS (sOCS) chamber, which allowed for spatial separation of the droplets in cavities with the dimensions 100 µm × 100 µm × 100 µm (see Fig. 4 below). The cavities were arranged as an array of 29×60 wells, thus leading to 1740 storage positions. Droplets generated in this system with flow rates of Q_{cont} = 30 µL min^{-1} and Q_{disp} = 0.5 µL min^{-1} were collected in the cavities. The dispersed phase consisted of DI water, 5 % (w/v) bovine serum albumin (BSA) supplemented with the enhanced green fluorescent protein (eGFP; 5 µM), which was produced by recombinant expression as described previously [24, 25]. In a typical experiment, all cavities were filled with droplets in less than 3 min and the droplets were then analyzed at 37 °C under stopped flow conditions by fluorescence microscopy over a period of 180 min. The droplet volumes and eGFP concentrations were determined from the images by using Fiji software.

3 Results and Discussion

3.1 Off-Chip Storage

For long term incubation of microfluidic W/O droplets, suitable storage containers are required into which the droplets can be easily transferred, and also removed from after storage. In this work, we investigated three different storage devices with regard to their suitability for maintaining the structural integrity of the droplets during the transfer and storage processes. As shown in Fig. 1, droplets were stored in an Eppendorf reaction cup (Fig. 1 b) or a PTFE tube (Fig. 1 c) or in the VDS structure (Fig. 1 d). All three variants were sealed tightly so that evaporation of reagents was kept at a minimum.

To analyze the structural integrity of the droplets during transfer and storage, their sizes and size distributions were determined immediately after generation in the flow focusing structure, as well as after transferal to the storage device and back transfer into the OCS chamber (Fig. 3). The volumes and coefficient of variation (CV) of the droplets were measured ($N \geq 100$). The data clearly shows that all droplets were highly monodisperse immediately after generation (black bars in Fig. 3) and thus had only minor deviations in their size (CV < 3 %; see also Tab. 1). The average droplet size was about 145 µm in diameter; however, the absolute droplet size varied in respective experiments due to slight variations in the manufacturing of the PDMS structures and in the flow rates [26]. For example, changing the flow rate of the dispersed phase from 1 to 7 µL min^{-1}, while keeping the continuous phase flow rate constant, resulted in an increase of the droplet diameter of about 17 %. As another example, by applying intentionally high forces when clamping the PDMS chip, the channel width of the flow focusing intersection changed from 100 to 92 µm, thus leading to an increase in the droplet diameter of about 20 %.

The droplet volume distributions after transfer to the storage device and back transfer into the OCS chamber (red bars in Fig. 2) indicated a reduction of the droplet volume for all three

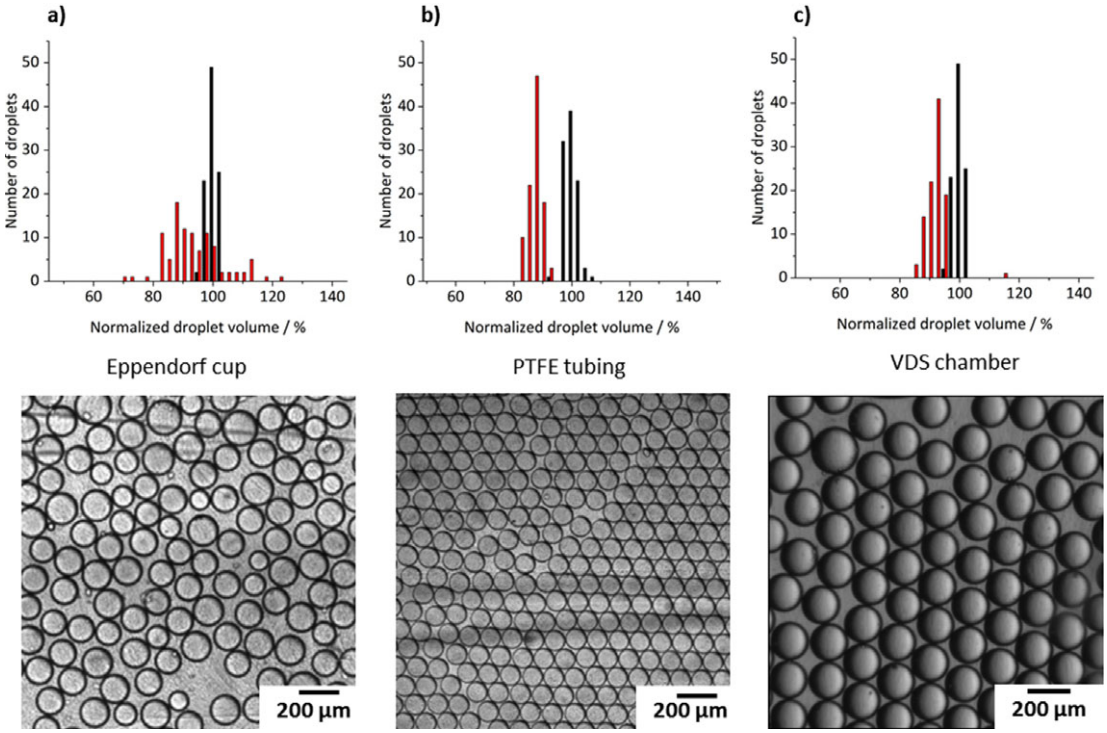

Figure 3. Frequency distribution of the droplet volume determined either directly after generation (black bars) or after transfer into the storage device and back-transfer into the OCS chamber (red bars): (a) Eppendorf cup, (b) PTFE tubing, (c) VDS chamber. The results were obtained from at least 100 droplets each. The images below show representative micrographs of respective W/O droplets taken after storage and back-transfer into the OCS structure.

storage variants. The normalized average droplet volume for the PTFE tubing decreased the most to 86.7 ± 2.3 % of the ini tial volume. The second highest shrinkage rate was observed in the VDS chamber with 91.7 ± 3.5 %. The lowest shrinkage after off chip incubation was observed for the Eppendorf cup (93.2 ± 9.4 %.) Nevertheless, with a standard deviation of 9.4 %, the storage in the Eppendorf cup led to the largest changes in the droplet volumes after the back transfer. These results are confirmed by the determination of the CV values (Tab. 1). While the droplets were highly monodisperse during droplet generation, monodispersity (CV ≥ 10) was no longer given after storage in the Eppendorf tube. In contrast, the other two methods allowed the droplets to maintain their monodispersity after back transfer, with the storage in PTFE tubing being accompanied by the smallest change.

Table 1. CV values of the W/O droplet sizes before (CV1) and after (CV2) storage.

	Eppendorf cup	PTFE tubing	VDS chamber
CV1 [%]	1.7	2.3	1.7
CV2 [%]	10.0	2.7	3.9

Since the tubing and off chip reservoirs were made of gas tight materials that should effectively prevent diffusion into the gas phase, and since the solubility of water in the hydrofluoro ether (HFE) 7500 oil is about 45 ppm (Datasheet Fluoridrop, Dolomite Microfluidics), diffusion of water molecules into the organic phase is a decisive factor for the observed shrinkage of the droplets [27]. However, quantitative estimations suggest that further processes, such as aqueous surfactant adsorbates at the droplet boundaries and solid surfaces, might play an im portant role as well. The smaller the volume of the organic phase around the water droplets, the faster this volume is satu rated and the lesser the droplets shrink [28]. Small droplets shrink more than larger droplets due to their higher surface to volume ratio [27]. The droplets in the PTFE tube initially have a smaller volume compared to the other two storage variants and therefore show greater shrinkage. In addition, the oil inside the PTFE tubing can flow continuously around the droplets in the tubing, such that water saturation occurs more slowly. Fur thermore, the large changes in CV observed for the droplets in the Eppendorf cup suggest that shear forces occurring during the transfer steps as well as spontaneous fusion of droplets and/or Ostwald ripening processes based on molecular diffu sion [29] can occur when the oil depleted physical barrier ex poses the droplets to each other.

3.2 On-Chip Storage

To avoid shear forces from droplet transfer and droplet coales cence upon storage, in situ on chip storage of the droplets was investigated with an OCS device that contained an sOCS cham ber. As an alternative to previously reported droplet storage

chips [30, 31], the sOCS chamber allowed for spatial separation of the droplets by collecting them in an array of 29×60 wells, thus leading to 1740 fixed storage positions (Fig. 4 a). The fixed storage provides the advantage of having positionally encoded W/O droplets to enable analysis of individual droplets and traceability in multiplex applications. Furthermore, the droplet fixation allows the continuous perfusion of the chamber with the oil phase, thus enabling analysis of the changes in individu al droplets depending on the continuous phase. While this mode of operation could be used, e.g., for crystallization or bio chemical experiments, we have here operated the device under static conditions to quantify the time dependent change in droplet size by diffusion of water into the oil phase [28].

To this end, the W/O droplets were produced in an sOCS chip mounted on a microscope stage that was preheated to 37 °C. To quantitatively investigate the effects on a dissolved biomolecular analyte, the dispersed phase contained the eGFP. The completely filled chamber was then incubated at 37 °C under stop flow conditions and images of the droplets were taken in 15 min intervals. It is clearly evident from the data shown in Fig. 4 b, c that the droplet volumes decreased steadily over 180 min time from 0.58 ± 0.07 nL to 0.41 ± 0.04 nL (ca. 30 %), while the fluorescence intensity remained constant. Hence, a monotonous increase in eGFP concentration occurred inside the droplets (Fig. 4 d). The observed shrinkage of the droplets can be attributed to the diffusion of the fluorocar boned oil along with the water inside the droplets into the PDMS structure and to evaporation processes, as discussed above. Since the entrapped eGFP protein cannot evaporate, this process leads to a time dependent concentration of the protein in the droplets. Due to the linearity of this process, this approach and our novel chip design should be particularly useful for the investigation of biochemical reactions and/or crystallization experiments.

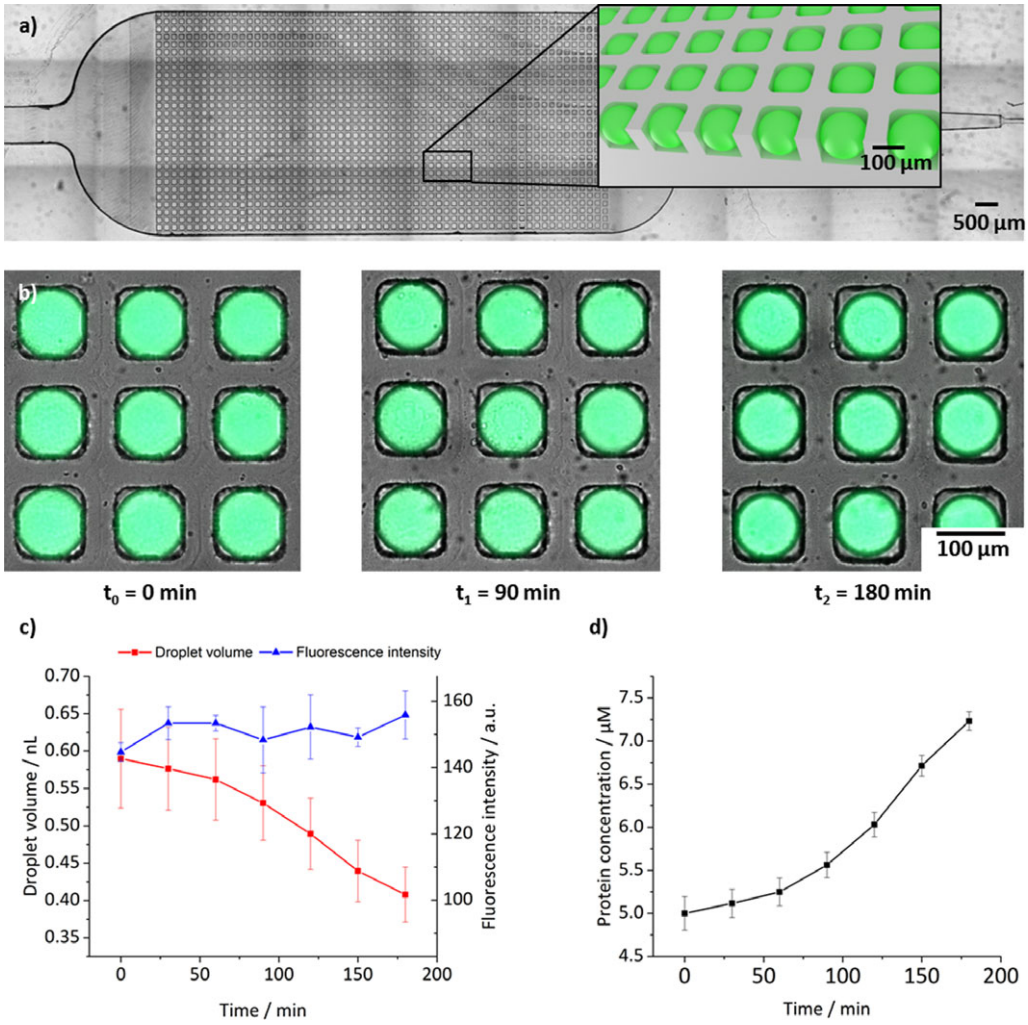

Figure 4. (a) Reflected light image of the sOCS device containing an array of 29×60 cavities. The inset shows a schematic representation of the W/O droplets inside the structure. (b) Representative overlay of fluorescence and reflected light images of W/O droplets inside the cavities obtained after variable times of storage (*t*). (c) Progression of the droplet volume (red) and the fluorescence intensity (blue) over time. (d) Development of the protein concentration in the droplet over time.

4 Conclusions

In summary, a systematic investigation is reported of three dif ferent storage devices with regard to their suitability for main taining the structural integrity of droplets during transfer and storage processes. The results clearly show that all methods led to a reduction in droplet volume, presumably due to diffusive behavior of water into the organic phase. Shear forces that can occur during the transfer process lead to a decrease or, in the case of Eppendorf cup storage, a complete loss of the droplet monodispersity. To avoid these forces and to control shrinkage upon storage, we here illustrate that in situ on chip storage of the droplets in a microcavity array can be used. The presented structure allows for spatially separated and thus positionally encoded droplet storage, thereby enabling the convenient anal ysis of individual droplets and their traceability in multiplex applications. Since we were able to show that the concentration of entrapped proteins can be increased by targeted droplet shrinkage, our approach should be well suited for numerous applications in the life sciences.

Acknowledgment

This research was funded by the Helmholtz program "BioInter faces in Technology and Medicine".

The authors have declared no conflict of interest.

Symbols used

CV	[%]	coefficient of variation
Q_{cont}	[$\mu L\,min^{-1}$]	flow rate of the continuous phase
Q_{disp}	[$\mu L\,min^{-1}$]	flow rate of the dispersed phase

Abbreviations

DI	deionized
eGFP	enhanced green fluorescent protein
HFE	hydrofluoroether
OCS	on chip storage
PDMS	polydimethylsiloxane
PMMA	polymethylmethacrylate
PP	polypropylene
PTFE	polytetrafluoroethylene
sOCS	structured on chip storage
VDS	vertical droplet storage
W/O	water in oil

References

[1] G. M. Whitesides, *Nature* **2006**, *442 (7101)*, 368 373. DOI: https://doi.org/10.1038/nature05058

[2] E. K. Sackmann, A. L. Fulton, D. J. Beebe, *Nature* **2014**, *507 (7491)*, 181 189. DOI: https://doi.org/10.1038/nature13118

[3] Y. Schaerli, F. Hollfelder, *Mol. Biosyst.* **2009**, *5 (12)*, 1392 1404. DOI: https://doi.org/10.1039/b907578j

[4] T. Schneider, J. Kreutz, D. T. Chiu, *Anal. Chem.* **2013**, *85 (7)*, 3476 3482. DOI: https://doi.org/10.1021/ac400257c

[5] C. Martino, A. J. deMello, *Interface Focus* **2016**, *6 (4)*, 20160011. DOI: https://doi.org/10.1098/rsfs.2016.0011

[6] D. Hummer, F. Kurth, N. Naredi Rainer, P. S. Dittrich, *Lab Chip* **2016**, *16 (3)*, 447 458. DOI: https://doi.org/10.1039/c5lc01314c

[7] P. C. Gach, K. Iwai, P. W. Kim, N. J. Hillson, A. K. Singh, *Lab Chip* **2017**, *17 (20)*, 3388 3400. DOI: https://doi.org/10.1039/c7lc00576h

[8] T. M. Squires, S. R. Quake, *Rev. Mod. Phys.* **2005**, *77 (3)*, 977 1026. DOI: https://doi.org/10.1103/RevModPhys.77.977

[9] Y. Liu, X. Jiang, *Lab Chip* **2017**, *17 (23)*, 3960 3978. DOI: https://doi.org/10.1039/c7lc00627f

[10] J. U. Shim, R. T. Ranasinghe, C. A. Smith, S. M. Ibrahim, F. Hollfelder, W. T. Huck, D. Klenerman, C. Abell, *ACS Nano* **2013**, *7 (7)*, 5955 5964. DOI: https://doi.org/10.1021/nn401661d

[11] D. R. Link, S. L. Anna, D. A. Weitz, H. A. Stone, *Phys. Rev. Lett.* **2004**, *92 (5)*, 054503. DOI: https://doi.org/10.1103/PhysRevLett.92.054503

[12] G. F. Christopher, J. Bergstein, N. B. End, M. Poon, C. Nguy en, S. L. Anna, *Lab Chip* **2009**, *9 (8)*, 1102 1109. DOI: https://doi.org/10.1039/b813062k

[13] X. Niu, S. Gulati, J. B. Edel, A. J. deMello, *Lab Chip* **2008**, *8 (11)*, 1837 1841. DOI: https://doi.org/10.1039/b813325e

[14] A. R. Abate, T. Hung, P. Mary, J. J. Agresti, D. A. Weitz, *Proc. Natl. Acad. Sci. USA* **2010**, *107 (45)*, 19163 19166. DOI: https://doi.org/10.1073/pnas.1006888107

[15] M. R. Bringer, C. J. Gerdts, H. Song, J. D. Tice, R. F. Ismagi lov, *Philos. Trans. R. Soc., A* **2004**, *362 (1818)*, 1087 1104. DOI: https://doi.org/10.1098/rsta.2003.1364

[16] H. D. Xi, H. Zheng, W. Guo, A. M. Ganan Calvo, Y. Ai, C. W. Tsao, J. Zhou, W. Li, Y. Huang, N. T. Nguyen, S. H. Tan, *Lab Chip* **2017**, *17 (5)*, 751 771. DOI: https://doi.org/10.1039/c6lc01435f

[17] G. Etienne, M. Kessler, E. Amstad, *Macromol. Chem. Phys.* **2017**, *218 (2)*, 1600365. DOI: https://doi.org/10.1002/macp.201600365

[18] L. J. Pan, J. W. Tu, H. T. Ma, Y. J. Yang, Z. Q. Tian, D. W. Pang, Z. L. Zhang, *Lab Chip* **2017**, *18 (1)*, 41 56. DOI: https://doi.org/10.1039/c7lc00800g

[19] J. B. Wacker, I. Lignos, V. K. Parashar, M. A. Gijs, *Lab Chip* **2012**, *12 (17)*, 3111 3116. DOI: https://doi.org/10.1039/c2lc40300e

[20] Y. Zhang, H. R. Jiang, *Anal. Chim. Acta* **2016**, *914*, 7 16. DOI: https://doi.org/10.1016/j.aca.2016.02.006

[21] C. J. Martinez, J. W. Kim, C. Ye, I. Ortiz, A. C. Rowat, M. Marquez, D. Weitz, *Macromol. Biosci.* **2012**, *12 (7)*, 946 951. DOI: https://doi.org/10.1002/mabi.201100351

[22] J. Clausell Tormos, D. Lieber, J. C. Baret, A. El Harrak, O. J. Miller, L. Frenz, J. Blouwolff, K. J. Humphry, S. Koster, H. Duan, C. Holtze, D. A. Weitz, A. D. Griffiths, C. A. Mert en, *Chem. Biol.* **2008**, *15 (5)*, 427 437. DOI: https://doi.org/10.1016/j.chembiol.2008.04.004

[23] J. Schindelin, I. Arganda Carreras, E. Frise, V. Kaynig, M. Longair, T. Pietzsch, S. Preibisch, C. Rueden, S. Saalfeld, B. Schmid, J. Y. Tinevez, D. J. White, V. Hartenstein, K. Eli ceiri, P. Tomancak, A. Cardona, *Nat. Methods* **2012**, *9 (7)*, 676 682. DOI: https://doi.org/10.1038/nmeth.2019

[24] F. Kukolka, C. M. Niemeyer, *Org. Biomol. Chem.* **2004**, *2 (15)*, 2203 2206. DOI: https://doi.org/10.1039/b406492e
[25] V. Lapiene, F. Kukolka, K. Kiko, A. Arndt, C. M. Niemeyer, *Bioconjugate Chem.* **2010**, *21 (5)*, 921 927. DOI: https://doi.org/10.1021/bc900471q
[26] T. Cubaud, T. G. Mason, *Phys. Fluids* **2008**, *20 (5)*, 053302. DOI: https://doi.org/10.1063/1.2911716
[27] M. Akhtar, S. van den Driesche, A. Bodecker, M. J. Velle koop, *Sens. Actuators, B* **2018**, *255*, 3576 3584. DOI: https://doi.org/10.1016/j.snb.2017.08.032
[28] M. He, C. Sun, D. T. Chiu, *Anal. Chem.* **2004**, *76 (5)*, 1222 1227. DOI: https://doi.org/10.1021/ac035196a
[29] T. Sakai, K. Kamogawa, K. Nishiyama, H. Sakai, M. Abe, *Langmuir* **2002**, *18 (6)*, 1985 1990. DOI: https://doi.org/10.1021/la0111248
[30] A. Huebner, D. Bratton, G. Whyte, M. Yang, A. J. deMello, C. Abell, F. Hollfelder, *Lab Chip* **2009**, *9 (5)*, 692 698. DOI: https://doi.org/10.1039/b813709a
[31] Y. D. Ma, K. Luo, W. H. Chang, G. B. Lee, *Lab Chip* **2018**, *18 (2)*, 296 303. DOI: https://doi.org/10.1039/c7lc01004d